Neoplasia • Vol. 9, No. 8, August 2007, pp. 662–670 662

www.neoplasia.com

Galectin-3 as a Potential Therapeutic Target in Tumors Arising from Malignant Endothelia[1]

Kim D. Johnson[*,†], *Olga V. Glinskii*[‡,§], *Valeri V. Mossine*[¶], *James R. Turk*[#], *Thomas P. Mawhinney*[¶], *Douglas C. Anthony*[**], *Carolyn J. Henry*[†,††], *Virginia H. Huxley*[‡], *Gennadi V. Glinsky*[‡‡], *Kenneth J. Pienta*[§§], *Avraham Raz*[¶¶] *and Vladislav V. Glinsky*[§,¶]

Departments of *Veterinary Pathobiology; [†]Veterinary Medicine and Surgery; [‡]Medical Pharmacology and Physiology, Hematology/Oncology Division, University of Missouri-Columbia, Columbia, MO 65211, USA; [§]Harry S. Truman Memorial Veterans' Hospital, Columbia, MO 65201, USA; Departments of [¶]Biochemistry; [#]Biomedical Sciences; **Pathology and Anatomical Sciences; [††]Internal Medicine, Hematology/Oncology Division, University of Missouri-Columbia, Columbia, MO 65211, USA; [‡‡]Translational and Functional Genomics Laboratory, Ordway Cancer Center, Ordway Research Institute, Albany, NY 12208, USA; [§§]Departments of Urology and Internal Medicine, University of Michigan Comprehensive Cancer Center, Ann Arbor, MI 48109, USA; [¶¶]Karmanos Cancer Institute, Wayne State University Medical School, Detroit, MI 48201, USA

Abstract

Angiosarcoma (ASA) in humans and hemangiosarcoma (HSA) in dogs are deadly neoplastic diseases characterized by an aggressive growth of malignant cells with endothelial phenotype, widespread metastasis, and poor response to chemotherapy. Galectin-3 (Gal-3), a β-galactoside–binding lectin implicated in tumor progression and metastasis, endothelial cell biology and angiogenesis, and regulation of apoptosis and neoplastic cell response to cytotoxic drugs, has not been studied before in tumors arising from malignant endothelia. Here, we tested the hypothesis that Gal-3 could be widely expressed in human ASA and canine HSA and could play an important role in malignant endothelial cell biology. Immunohistochemical analysis demonstrated that 100% of the human ASA (10 of 10) and canine HSA (17 of 17) samples analyzed expressed Gal-3. Two carbohydrate-based Gal-3 inhibitors, modified citrus pectin (MCP) and lactulosyl-L-leucine (LL), caused a dose-dependent reduction of SVR murine ASA cell clonogenic survival through the inhibition of Gal-3 antiapoptotic function. Furthermore, both MCP and LL sensitized SVR cells to the cytotoxic drug doxorubicin to a degree sufficient to reduce the *in vitro* IC_{50} of doxorubicin by 10.7-fold and 3.6-fold, respectively. These results highlight the important role of Gal-3 in the biology of ASA and identify Gal-3 as a potential therapeutic target in tumors arising from malignant endothelial cells.

Neoplasia (2007) **9,** 662–670

Keywords: Angiosarcoma, galectin-3, chemotherapy, doxorubicin, apoptosis.

Introduction

Human angiosarcoma (ASA) is a rare but deadly malignant vascular tumor that accounts for 1% to 2% of all sarcomas. ASA is aggressive and tends to recur locally, to spread widely, and to possess a high rate of lymph node and systemic metastases [1]. It is characterized by early local and systemic dissemination, restricting indications for surgical resection to a small number of patients. The treatment of human ASA can be challenging and futile [1]. Chemotherapy and radiation therapy may be indicated as either adjuvant or primary treatment, but their use is often limited by the poor physical condition of patients. The rate of tumor-related death in patients with ASA is high, with survival ranging from 6 to 9 months, regardless of the treatment chosen, and with the reported 5-year survival rate being < 20% [2–5].

Canine hemangiosarcoma (HSA) is a common fatal cancer of dogs arising from transformed vascular endothelial cells that resembles human ASA [6,7] and can serve as a model of metastatic ASA in humans [7]. HSA, which also has an endothelial phenotype, occurs more frequently in dogs than in any other species, comprising up to 5% to 7% of primary noncutaneous malignant neoplasms. This tumor affects almost every dog breed, but large-breed dogs and those that are lightly pigmented or sparsely haired appear to be at a higher risk. HSA can arise in any tissue with blood vessels, but the most common sites in dogs are the spleen (50–65%), right atrium/auricle (3–25%), subcutaneous tissues (13–17%), and the

Address all correspondence to: Vladislav V. Glinsky, MD, Department of Biochemistry, University of Missouri, M743 Medical Science Building, Columbia, MO 65212.
E-mail: glinskiivl@missouri.edu

[1]This work was supported by the VA Merit Review Program (V. V. Glinsky); a research grant from the Tom and Betty Scott Endowed Program in Veterinary Oncology (K. D. Johnson); National Institutes of Health (NIH) grant RO1 HL078816 and National Aeronautics and Space Administration grant NNJ05HF37G (V. H. Huxley); NIH grant 5RO1 CA89827 (G. V. Glinsky); NIH grants P50 CA69568 SPORE in Prostate Cancer and PO1 CA093900-01A2 (K. J. Pienta); and NIH grant R37 CA046120-19 (A. Raz). Kenneth J. Pienta is an American Cancer Society clinical research professor.
Received 21 May 2007; Revised 8 June 2007; Accepted 13 June 2007.

DOI 10.1593/neo.07433

liver (5–6%) [8]. Similar to human ASA, canine HSA is characterized by early and aggressive metastasis. Local infiltration and systemic metastasis are common growth patterns, and metastatic sites are widespread. Morbidity and mortality in dogs with HSA are often due to acute internal hemorrhage secondary to tumor rupture. Despite surgery and intensive chemotherapy, the median survival time for dogs is a little more than 6 months [8,9].

Based on poor response to available therapies, there is a need to identify molecular targets in ASA that would facilitate the development of novel mechanism-based therapeutic approaches. Spontaneously developing canine HSA could serve as a model system for validating these targets and for testing new therapeutic modalities. Here, we suggest that one such potential target could be galectin-3 (Gal-3; $M_r \sim 31$ kDa), a member of the family of mammalian carbohydrate-binding proteins with an affinity to terminal β-galactose and with highly conserved features in the carbohydrate-binding domain [10]. Gal-3 is prominently expressed in a variety of neoplasms, including stomach [11,12], colon [13], breast [14], bladder [15,16], and thyroid [17] cancers. This carbohydrate-binding protein is involved in many physiological and pathological processes, such as cell growth and differentiation [18,19], cell–cell and cell–extracellular matrix adhesions [20], metastasis [21], and regulation of apoptosis [18,22–26]. Furthermore, Gal-3 has been shown to control tumor cell sensitivity to chemotherapy through the regulation of apoptotic responses to cytotoxic drugs [23]. In several experimental systems, Gal-3 expression has been associated with increased malignant and metastatic phenotype [24–28]. In addition, Gal-3 is intimately involved in endothelial biology and angiogenesis [29], as well as in endothelial cell morphogenesis [29]. To date, however, Gal-3 has not been studied in tumors arising from malignant endothelia, such as human ASA and/or canine HSA.

Given the importance of this carbohydrate-binding protein in both malignant transformation and endothelial cell biology, we hypothesize that Gal-3 could be prominently expressed in tumors arising from malignant endothelia and could serve as a potential therapeutic target in these neoplasms. Here, we tested this hypothesis by analyzing Gal-3 expression in archived specimens of human ASA and canine HSA, and by investigating the consequences of inhibiting Gal-3 function in a murine HSA cell line using two carbohydrate-based Gal-3 inhibitors, modified citrus pectin (MCP) [29–31] and lactulosyl-L-leucine (LL) [32,33].

Materials and Methods

Chemicals and Reagents

All chemicals and reagents were of analytic grade and, unless otherwise specified, were from Sigma Chemical Co. (St. Louis, MO). The hybridoma cell line TIB-166, which produces rat monoclonal anti–Gal-3 antibody, was obtained from the American Type Culture Collection (ATCC; Manassas, VA). The preparation of MCP and LL has been described elsewhere [29–33]. The carbohydrate specificity of LL and MCP has been investigated previously. Specifically, the carbohydrate specificity of MCP anti–Gal-3 effect was controlled using lactose, sucrose, and unmodified citrus pectin [31]. The carbohydrate specificity of LL anti–Gal-3 action was controlled using lactose and maltose [21]. Furthermore, in one of the earlier studies [20], we specifically synthesized as a control compound for LL the glycoamine lactitol-L-leucine, which differs from LL only in that glucose in lactitol is in open (alcohol) form; this modification completely abrogated the compound's anti–Gal-3 activity.

Tissue Samples

Archived formalin-fixed paraffin-embedded (FFPE) tissues from 10 surgically removed human ASA from the University of Missouri Healthcare System and 17 canine HSA from the University of Missouri Veterinary Medical Diagnostic Laboratory (VMDL) were used for Gal-3 expression and immunohistochemical analyses. Normal canine tissues from patients without HSA at the VMDL were also analyzed.

Cancer Cell Lines and Cultures

The murine HSA cell line SVR was obtained from the ATCC. This cell line was developed from murine endothelial cells isolated from pancreatic islets of C57BL/6 adult mice, which were transduced with a retrovirus encoding H-ras and hygromycin resistance [34]. SVR cells were grown as monolayers on plastic at 37°C in a 5% CO_2/95% air atmosphere using RPMI 1640 supplemented with 10% fetal bovine serum, L-glutamine, and gentamycin, and subcultured every 2 to 3 days.

Immunohistochemistry

Gal-3 protein was localized in FFPE tissue sections of human ASA and canine HSA by immunohistochemistry using a 1:100 dilution of rat primary monoclonal anti–Gal-3 antibody TIB-166. Briefly, deparaffinized and steamer-treated sections were treated with 3% hydrogen peroxide for 10 minutes to block endogenous peroxidase. Following an avidin–biotin block (SP2001; Vector, Burlingame, CA), a rinse with Tris buffer (TB), and a 10-minute protein block (XO 909; Dako, Carpinteria, CA), the sections were incubated with primary anti–Gal-3 antibody overnight at 4°C (1:100 dilution). On the following morning, slides were rinsed in TB and incubated with rabbit anti-rat IgG (1:1500 dilution, A5795; Sigma) for 30 minutes at room temperature. After an additional rinse with TB, a Link step ($LSAB^+$; Dako) for 30 minutes at room temperature, and another TB rinse and Label step ($LSAB^+$; Dako) for 30 minutes, the slides were washed thoroughly with distilled water and incubated with 3,3′-diaminobenzidine (K3466; Dako) for 5 to 10 minutes at room temperature. Hematoxylin counterstaining was performed, followed by dehydration and coverslipping. Negative controls consisted of omission of the primary antibody. Endothelial cell phenotype was identified by immunostaining the sections with a 1:800 dilution of primary rabbit polyclonal antibody and von Willebrand factor. In spleen samples, brown granules of hemosiderin were identified with Prussian blue stain for iron. For analyzing Gal-3 expression in the

murine SVR HSA cell line, the cells were grown until 60% to 80% confluent directly on microscope slides using the chamber slide system (NalgeNunc, Naperville, IL). After fixing and permeabilizing cells overnight in 2% formaldehyde solution in phosphate-buffered saline (PBS), Gal-3 immunostaining was performed exactly as described for ASA and HSA samples (see above), including negative control omitting the primary antibody, counterstaining, and coverslipping.

Computer-Assisted Image Analysis

Sections were photographed with an Olympus BX60 photomicroscope (Olympus, Center Valley, PA) and Spot Insight Color digital camera (Diagnostic Instruments, Sterling Heights, MI). The area of positive staining for Gal-3 was calculated as a percentage of the total section area using ImageProPlus software (Media Cybernetics, Bethesda, MD).

Clonogenic Survival

SVR cells, grown until 50% to 60% confluent, were harvested using a nonenzymatic cell dissociation reagent and pipetted to produce a single-cell suspension. Next, cells were plated at low density (200 cells/well) in quadruplicate in 24-well culture plates without (control) or with indicated concentrations of the compounds tested. Seven days later, the cells were fixed with 2% formaldehyde in PBS and stained with hematoxylin, and colonies of $\geq$ 15 cells were scored. Only cells with a viability of $\geq$ 95%, as determined by trypan blue dye exclusion, were used for these experiments.

Apoptosis Induction Experiments

Apoptosis studies were performed using the TdT-mediated deoxyuridine triphosphate nick end labeling (TUNEL) method. SVR cells, grown until 50% to 60% confluent, were harvested using a nonenzymatic cell dissociation reagent and pipetted to produce a single-cell suspension. Next, SVR cells were plated at low density (200 cells/well) in quadruplicate using four-well chamber slides without (control) or with Gal-3 inhibitors tested (LL at 1.0 mM, or MCP at a final concentration of 0.25%). After 24 hours, the cells were fixed in 2% formaldehyde in PBS. TUNEL assay was performed using the *in situ* Cell Death Detection kit POD (Roche Diagnostics, Indianapolis, IN) according to the manufacturer's protocol, and apoptotic and nonapoptotic cells were scored.

Western Blot Analysis

SVR cells, grown until 50% to 60% confluent, were harvested, washed with PBS, and resuspended with cell lysis buffer (C3228; Sigma) supplemented with protease inhibitor cocktail (P8340; Sigma) at a ratio of 1:10 (vol/vol). The suspension was centrifuged at 10,000 rpm for 10 minutes. Protein concentrations were determined using protein assay reagent (Bio-Rad, Hercules, CA). A 30-μg aliquot of the total cellular protein was resolved on a 10% Nu Page Bis Tris gel (Invitrogen, Carlsbad, CA). Proteins were transferred onto a nitrocellulose membrane (Invitrogen). After blocking with 5% nonfat milk, membranes were reacted with the anti–Gal-3 antibody at a 1:200 dilution, followed by goat anti-rat IgG secondary antibody conjugated to horseradish peroxidase (A5795; Sigma) at a 1:8000 dilution in 5% nonfat milk in Tris-buffered saline Tween-20 solution. Expression levels were detected using chemical luminescence (Enhanced Chemical Luminescence, RPN 2132; Amersham, Piscataway, NJ).

Statistical Analysis

Statistical analysis of data was performed using GraphPad Prism version 4 software (GraphPad Software, Inc., San Diego, CA). Two-tailed *t*-test was used to assess the statistical significance of data. Bar graphs represent mean ± standard deviation. The significance level was set at $P < .05$.

Results

Gal-3 Expression in Human ASA and Canine HSA

Routine immunohistochemical labeling protocols were used to detect Gal-3 in FFPE tissue sections of human ASA and canine HSA using TIB-166 anti–Gal-3 monoclonal antibody. We evaluated the expression of Gal-3 in 10 archived human ASA and 17 canine HSA samples (Figure 1). The intensity of Gal-3 immunolabeling was evaluated semiquantitatively by three independent observers (K.D.J., J.R.T., and V.V.G.) as follows: (0) negative; (1+) 1% to 10% positive cells; (2+) 10% to 50% positive cells; and (3+) 50% to 100% positive cells. One hundred percent (10 of 10 human cases and 17 of 17 canine cases) of the specimens tested were positive for Gal-3. These results are summarized in Tables 1 and 2.

In addition, we performed computer-assisted image analyses (Figure 1, *E*–*H*) using ImageProPlus software for quantification of Gal-3 expression in tumor tissues *versus* negative controls. The results of computer-assisted analyses correlated well with the scores made by the observers in samples with high (3+) and moderate (2+) Gal-3 expressions. In samples with negative (0) or weak (1+) Gal-3 expression, however, computer-assisted analyses often yielded elevated (false positive) scores.

In the majority of cases, hematoxylin and eosin (H&E) staining (Figure 2*A*), Gal-3 staining (Figure 2*B*), nonimmune control (Figure 2*C*), and factor VIII–related antigen (von Willebrand factor) staining (Figure 2*D*) were sufficient for characterizing samples and for analyzing the level of Gal-3 expression. However, in canine cases associated with HSA localization in the spleen, brown staining was also observed in normal spleen tissue even on H&E slides (Figure 2*E*, *black arrows*) and in nonimmune controls (Figure 2*G*, *red arrows*). As hemosiderin (an iron pigment resulting from hemoglobin degradation) is common in canine spleen tissue, we suggested that this brown staining in H&E and nonimmune samples of normal canine spleen belongs to hemosiderin deposits. Indeed, this suggestion was easily confirmed using iron staining (Figure 2*H*, *green arrows*). This differential diagnostic approach is most relevant to canine HSA, where the spleen is the most common site. It is irrelevant and un-

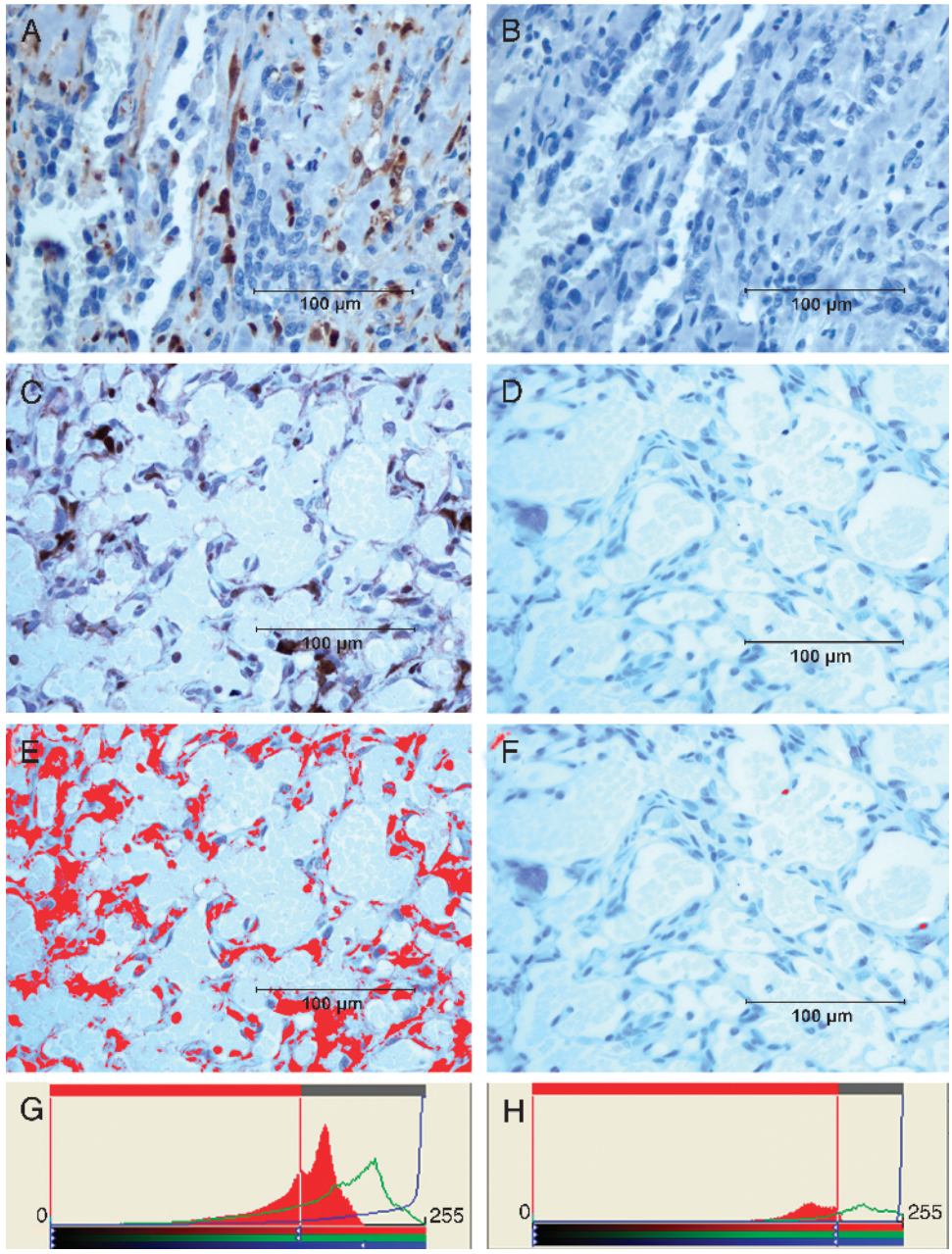

Figure 1. *Immunohistochemical analysis of Gal-3 expression using TIB-166 rat anti–Gal-3 monoclonal antibody in human ASA (A and B) and canine HSA (C and D). Brown staining in (A) and (C) represents Gal-3 immunoreactivity. (B) and (D) show corresponding negative controls omitting a primary antibody. (E–H) An example of the computer-assisted analysis of images shown in (C) and (D) using ImageProPlus software. The results of a computer-assisted analysis correlated well with the scores made by the observers in samples with high and moderate Gal-3 expressions. However, in samples with negative or weak Gal-3 expression, computer-assisted analysis yielded often elevated (false-positive) scores. Slides were counterstained with hematoxylin. Scale bars, 100 μm.*

Table 1. Expression of Gal-3 in Human ASA Specimens.

ASA Specimens		Number of Specimens Showing the Slated Degree of Immunoreactivity			
Location	Number Examined	0	1+	2+	3+
Skin	3	0	1	2	0
Bone	1	0	0	0	1
Scalp	1	0	0	0	1
Breast	2	0	0	0	2
Ileum	1	0	1	0	0
Liver	2	0	0	1	1
Total	10	0	2	3	5

Table 2. Expression of Gal-3 in Canine HSA Specimens.

HSA Specimens		Number of Specimens Showing the Slated Degree of Immunoreactivity			
Location	Number Examined	0	1+	2+	3+
Spleen	6	0	2	3	1
Omentum	1	0	1	0	0
Skin	6	0	4	2	0
Muscle	2	0	1	0	1
Bone	2	0	2	0	0
Total	17	0	10	5	2

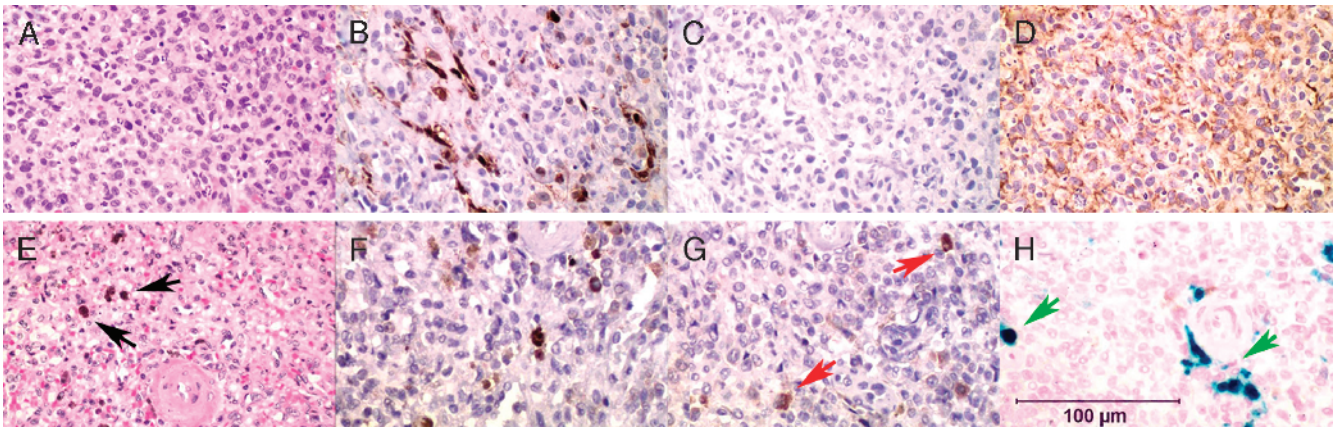

Figure 2. *Differential diagnosis between Gal-3 and hemosiderin staining in canine splenic HSA samples. In (A)–(D), an HSA sample was characterized using H&E staining (A), anti–Gal-3 antibody (B), nonimmune control (C), and anti–von Willebrand factor polyclonal antibody (D). Brown staining in (B) indicates Gal-3 immunoreactivity. Brown staining in (D) shows von Willebrand factor immunoreactivity consistent with the endothelial origin of HSA cells. In (E)–(H), a sample of normal canine spleen tissue is shown. Note the presence of brown staining material in H&E slides (E, black arrows) and nonimmune control (G, red arrows) identified as hemosiderin deposits using Prussian blue stain for iron (H, green arrows). Scale bar shown in (H), 100 μm.*

necessary, however, in human ASA, which occurs most commonly in cutaneous tissues.

Consequences of Gal-3 Inhibition in Malignant Endothelial Cells

Next, we investigated whether Gal-3 expression in malignant endothelial cells plays a significant biologic role in tumor cell growth and survival *in vitro*. We have used two carbohydrate-based Gal-3 inhibitors, MCP [29–31] and LL [32,33], to evaluate their effects on malignant endothelial cell clonogenic survival and growth, as well as on tumor cell sensitivity to chemotherapy. In these experiments, due to the unavailability of human ASA cell lines, we used murine SVR ASA cells [34]. First of all, we investigated whether, similarly to human ASA and canine HSA, murine SVR cells express Gal-3. Both immunohistochemical (Figure 3*A*) and Western blot (Figure 3*B*) analyses demonstrated that SVR cells express significant Gal-3 amounts.

After confirming the presence of our target protein in SVR cells, we investigated how various concentrations of MCP and LL affected the clonogenic survival and growth of SVR cells. In clonogenic survival experiments, we plated SVR ASA cells at low density (200 cells/well in 24-well plates) in various concentrations of either MCP (0–0.5%) or LL (0–1.0 mM). Seven days later, colonies of $\geq$ 15 cells were scored. The results of these experiments (Figure 4, *A–C*) demonstrated that both carbohydrate-based Gal-3 inhibitors reduced the clonogenic survival of SVR cells in a dose-dependent manner.

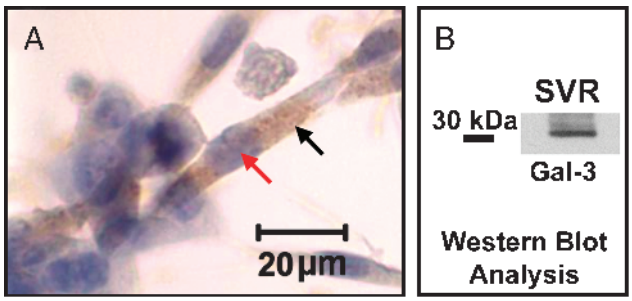

Figure 3. *Immunohistochemical analysis (A) and Western blot analysis (B) confirmation of Gal-3 expression in the murine ASA cell line SVR. In (A), brown staining indicates Gal-3 immunoreactivity. Note the predominantly cytoplasmic Gal-3 localization (black arrow) with limited nuclear positivity (red arrow). In (B), a single Gal-3 immunoreactive band was identified by Western blot analysis.*

When tumor cells are plated at low density as in clonogenic survival assays, the majority of cells die by execution of apoptosis, with only a small fraction surviving and giving rise to new clones. Thus, we suggested that the inhibitory effect of MCP and LL on clonogenic survival is likely due to the inhibition of a Gal-3 antiapoptotic function. Indeed, when we performed TUNEL assay 24 hours after plating SVR cells for clonogenic survival, we found that both MCP and LL reduced significantly the percentage of TUNEL-negative (nonapoptotic) cells compared to untreated controls (Figure 4, *D–F*). These results indicate that the effect of the carbohydrate-based Gal-3 inhibitors MCP and LL on HSA cells is associated, in part, with a decrease in tumor cells' ability to resist apoptosis.

This outcome naturally led us to the next hypothesis. Because the majority of currently used cytotoxic drugs act on cancer cells by inducing apoptosis and because the carbohydrate-based Gal-3 inhibitors MCP and LL reduce tumor cell resistance to apoptosis, we hypothesized that Gal-3 inhibitors would increase the sensitivity of neoplastic cells to cytotoxic drugs. To test this hypothesis, we investigated next whether MCP and LL sensitize ASA cells to doxorubicin, a chemotherapeutic drug commonly used to treat canine HSA. From clonogenic survival experiments, we determined the IC_{min} (the minimal concentration of a drug causing a statistically significant effect) for MCP and LL at 0.06% and 200 μM, respectively. When applied at IC_{min}, MCP and LL caused ~30% and ~20% inhibition of SVR clonogenic survival, respectively. Next, we used clonogenic

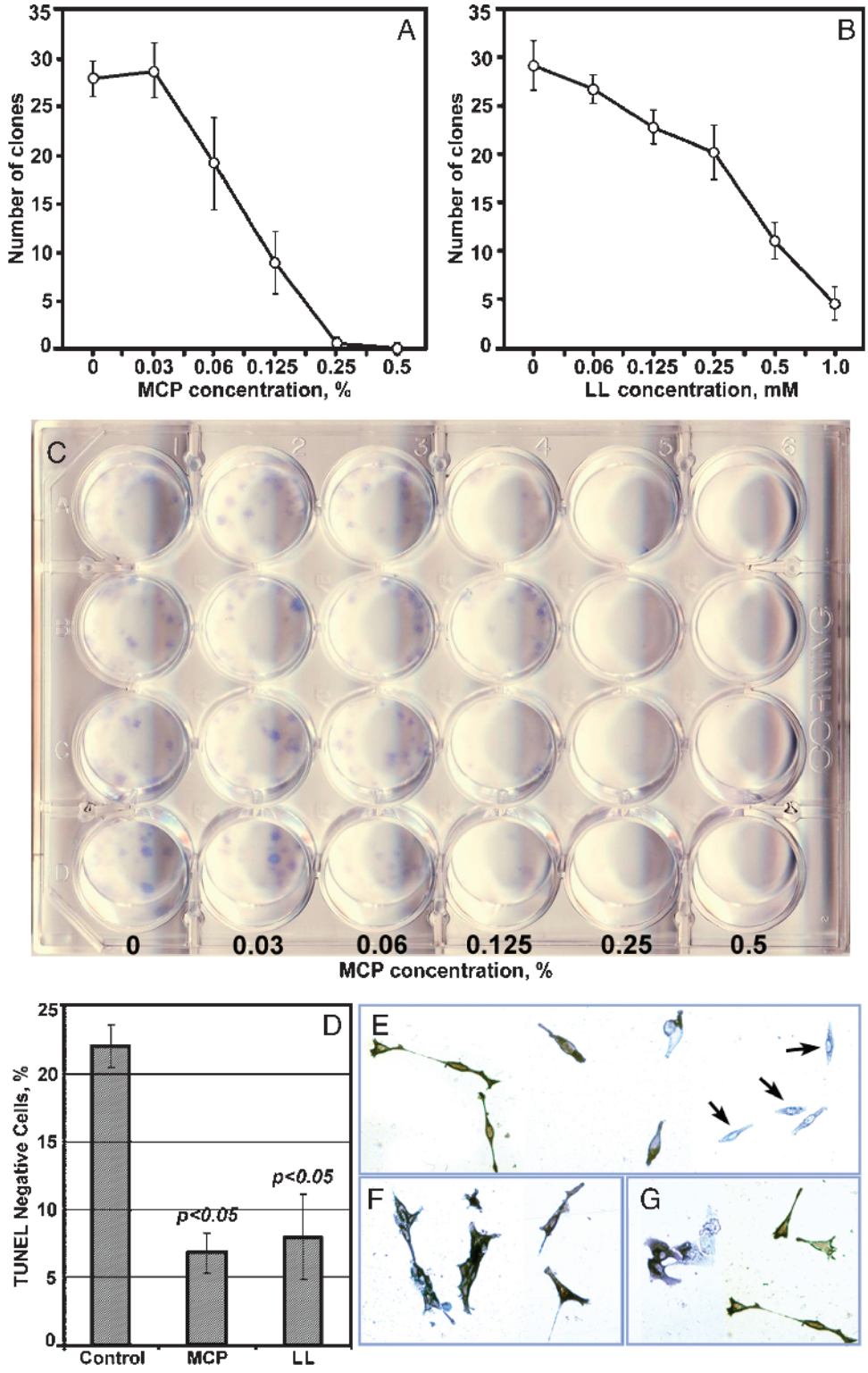

Figure 4. *The effect of the small-molecular-weight carbohydrate-based Gal-3 inhibitors MCP and LL on the clonogenic survival of SVR cells. In (A)–(C), SVR cells were plated at low density (200 cell/well) in 24-well plates in increasing concentrations of MCP (0–0.5%) and LL (0–1 mM). Seven days later, colonies of ≥ 15 cells were scored. Both MCP (A and C) and LL (B) inhibited the clonogenic survival of SVR cells in a dose-dependent manner. TUNEL analysis (D–G) demonstrated that the effect of both MCP (D and F) and LL (D and G) on SVR clonogenic survival was associated with a significant reduction in the percentage of TUNEL-negative (nonapoptotic) cells in samples treated with MCP (F) and LL (G) compared to untreated control (E). Note the presence of nonapoptotic cells in the untreated control (E, black arrows)* versus *an almost complete absence of TUNEL-negative cells in samples treated with MCP (F) or LL (G).*

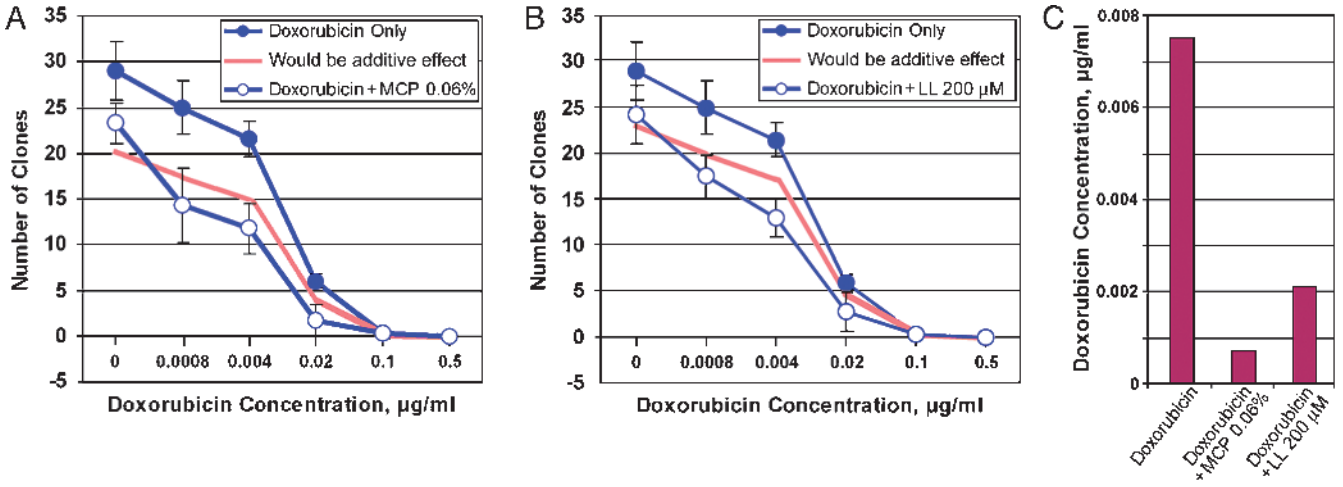

Figure 5. *The effect of the carbohydrate-based Gal-3 inhibitors MCP and LL on SVR cell sensitivity to doxorubicin. Both MCP (A) and LL (B) sensitize SVR cells to doxorubicin. Note the significant shift to the left of graphs representing a combined effect of doxorubicin with the IC_{min} of MCP (A, open circles) and LL (B, open circles) compared to the effect of doxorubicin alone (A and B, closed circles), or a would-be-additive-effect graph (A and B, red line) on the clonogenic survival of SVR. (C)* In vitro *IC_{50} of doxorubicin alone or in combination with the IC_{min} of MCP (0.06%) or LL (200 µM).*

survival assay to titrate the effect of doxorubicin on SVR cells alone or on the background of the IC_{min} of MCP or LL. As expected, doxorubicin alone inhibited the clonogenic survival of SVR cells in a dose-dependent manner (Figure 5), and this effect was even greater when doxorubicin was used in combination with the IC_{min} of MCP (Figure 5*A*) or LL (Figure 5*B*). To determine whether the enhanced inhibition of SVR clonogenic survival noted after a combined application of doxorubicin and carbohydrate-based Gal-3 inhibitors resulted from a simple summation of their respective effects as single agents, or whether MCP and LL indeed sensitized ASA cells to doxorubicin, we generated a projected "would-be-additive-effect" line by extrapolating the effects of MCP and LL IC_{min} to the doxorubicin dose-dependent effect (Figure 5, *A* and *B*, *red line*). For both compounds, the graphs representing the actual combined effects of doxorubicin with MCP and LL were significantly shifted to the left compared to would-be-additive-effect graphs (Figure 5, *A* and *B*), providing evidence that both MCP and LL synergize with doxorubicin by sensitizing ASA cells to this chemotherapeutic drug. Indeed, this sensitization was sufficient to reduce doxorubicin IC_{50} by 10.7-fold (0.0075–0.0007 µg/ml) and 3.6-fold (0.0075–0.0021 µg/ml) by MCP and LL, respectively (Figure 5*C*).

Discussion

Identifying new molecular targets for cancer therapy, including mechanism-based combination therapy, may lead to more potent synergistic effects on tumor growth and metastasis. In recent years, a β-galactoside–binding lectin, Gal-3, has attracted increasing attention as a potential therapeutic target in several cancers, such as breast cancer [14,19,20,31], prostate cancer [19,20,30], colon cancer [31], gastric cancer [11,12], and multiple myeloma [35]. Here, we demonstrated that Gal-3 is expressed widely in human and canine tumors arising from malignant endothelia and could be targeted efficiently by the small-molecular-weight carbohydrate-based inhibitors MCP and LL. Until recently, MCP and LL were studied mostly for their potential to control and prevent hematogenous cancer metastasis through inhibition of Gal-3–mediated metastatic cell homotypic and heterotypic aggregation and adhesion [19,20,30,31,33]. Recent experimental evidence demonstrating that Gal-3 is also an important regulator of programmed cell death with potent anti-apoptotic activity [10,23–26] suggests that these same inhibitors may have potential to sensitize neoplastic cells to cytotoxic drug–induced apoptosis, thus enhancing their antineoplastic effects on cancer cells. Although the precise molecular mechanisms by which Gal-3 exerts its antiapoptotic function are not understood, several key molecular and cellular events associated with this process have been identified. It has been shown that, in response to apoptosis induced by cytotoxic drugs (including doxorubicin, which was used in this study), Gal-3 translocates from the nuclei (where it undergoes phosphorylation by casein kinase 1 at Ser^6) to the cytoplasm [25], specifically to perinuclear membranes [26], where it effectively protects mitochondrial integrity, prevents cytochrome *c* release [26], and downregulates caspase cascade [24–26]. At least two distinct molecular pathways, activation of mitogen-activated protein kinase (ERK and JNK) pathways [25] and downregulation of Bad expression accompanied by increased Bad phosphorylation [24], are ultimately involved in Gal-3 antiapoptotic action. Based on this information, it appears that, to inhibit Gal-3 antiapoptotic effects, carbohydrate-based compounds such as MCP and LL interact with intracellular Gal-3. Indeed, extracellular Gal-3 does not protect cancer cells from apoptosis [26]. This may explain why anti–Gal-3 antibody only blocks Gal-3–mediated adhesion [36] but does not inhibit Gal-3 antiapoptotic function. It appears that smaller-molecular-weight carbohydrate-based compounds are required to interact with intracellular Gal-3. Thus, using small-molecular-weight carbohydrate-based compounds for inhibiting Gal-3 antiapoptotic function may represent a new

exciting approach for augmenting cytotoxic drug effects on cancer cells. Indeed, recent work from Chauhan et al. [35] has demonstrated that MCP sensitizes multiple myeloma cells to cytotoxic drugs by inhibiting Gal-3 antiapoptotic function in the mitochondrial apoptosis pathway. Similarly, it appears that the mechanism of the antineoplastic effect of the carbohydrate-based Gal-3 inhibitors MCP and LL on ASA cells is also associated, in part, with the inhibition of Gal-3 antiapoptotic function in malignant endothelial cells. Consequently, both MCP and LL reduce the clonogenic survival of ASA cells and increase their sensitivity to doxorubicin-induced apoptosis. This sensitization is sufficient to cause a 10.7-fold and 3.6-fold reduction in the IC_{50} of doxorubicin by MCP and LL, respectively.

Because of the limitations of surgery, the chemotherapeutic agent doxorubicin is currently the standard of care for dogs with HSA. However, even for dogs diagnosed with early-stage disease and undergoing chemotherapy, the 1-year survival rate rarely exceeds 10%. The cumulative cardiotoxic effects of doxorubicin on dogs and humans limit the ability to escalate drug dose in the hopes of improving its antitumor efficacy. Inhibition of antiapoptotic proteins, such as Gal-3, in cancer cells offers the promise of increasing the efficacy of doxorubicin and other chemotherapeutics while reducing their associated toxicities.

Currently, different groups explore multiple approaches to improving the efficacy of radiation therapy and chemotherapy on cancer cells. For example, the potential for increasing the effect of radiation therapy by inhibiting oncogenic K-Ras signaling is actively explored [37]. Various strategies for inhibiting antiapoptotic Bcl-2 family members to enhance tumor cell apoptotic responses to chemotherapy are being developed [38,39]. Galectins are emerging as promising molecular targets for cancer therapy, and galectin inhibitors might have the potential to be used as antitumor and antimetastatic agents. Targeting cancer cell adhesive interactions mediated by Gal-3 and its binding partner Thomsen-Friedenreich antigen using function-blocking antibodies efficiently inhibited metastatic cancer spread *in vivo* [40]. In addition to that, it appears that carbohydrate-based anti–Gal-3 therapies show promise for the treatment of cancer by enhancing the effects of cytotoxic drugs. A better understanding of the role of galectins in cancer might lead to novel clinical applications for diagnostic and therapeutic purposes. With these, the use of spontaneously developing tumors in large mammalian species (such as dogs) as models for testing new therapeutic strategies and modalities has been increasingly appreciated in recent years [7,41]. Thus, the results presented in this study warrant further expansion of this work to a species with naturally occurring HSA, such as dogs, which may serve as an invaluable model for the development and evaluation of new therapeutic strategies.

References

[1] Morgan MB, Swann M, Somach S, Eng W, and Smoller B (2004). Cutaneous angiosarcoma: a case series with prognostic correlation. *J Am Acad Dermatol* **50**, 867–874.

[2] Fedok FG, Levin RJ, Maloney ME, and Tipirneni K (1999). Angiosarcoma: current review. *Am J Otolaryngol* **20**, 223–231.

[3] Mendenhall WM, Mendenhall CM, Werning JW, Reith JD, and Mendenhall NP (2006). Cutaneous angiosarcoma. *Am J Clin Oncol* **29**, 524–528.

[4] Pawlik TM, Paulino AF, McGinn CJ, Baker LH, Cohen DS, Morris JS, Rees R, and Sondak VK (2003). Cutaneous angiosarcoma of the scalp: a multidisciplinary approach. *Cancer* **98**, 1716–1726.

[5] Selim A, Khachemoune A, and Lockshin NA (2005). Angiosarcoma: a case report and review of the literature. *Cutis* **76**, 313–317.

[6] Akhtar N, Padilla ML, Dickerson EB, Steinberg H, Breen M, Auerbach R, and Helfand SC (2004). Interleukin-12 inhibits tumor growth in a novel angiogenesis canine hemangiosarcoma xenograft model. *Neoplasia* **6**, 106–116.

[7] Fosmire SP, Dickerson EB, Scott AM, Bianco SR, Pettengill MJ, Meylemans H, Padilla M, Frazer-Abel AA, Akhtar N, Getzy DM, et al. (2004). Canine malignant hemangiosarcoma as a model of primitive angiogenic endothelium. *Lab Invest* **84**, 562–572.

[8] Thamm DH (2007). Miscellaneous tumors: hemangiosarcoma. In *Small Animal Clinical Oncology*. SJ Withrow and DM Vail (Eds). Saunders: St. Louis, MO. pp. 785–795.

[9] Clifford CA, Mackin AJ, and Henry CJ (2000). Treatment of canine hemangiosarcoma: 2000 and beyond. *J Vet Intern Med* **14**, 479–485.

[10] Akahani S, Nangia-Makker P, Inohara H, Kim HR, and Raz A (1997). Galectin-3: a novel antiapoptotic molecule with a functional BH1 (NWGR) domain of Bcl-2 family. *Cancer Res* **57**, 5272–5276.

[11] Baldus SE, Zirbes TK, Weingarten M, Fromm S, Glossmann J, Hanisch FG, Monig SP, Schroder W, Flucke U, Thiele J, et al. (2000). Increased galectin-3 expression in gastric cancer: correlations with histopathological subtypes, galactosylated antigens and tumor cell proliferation. *Tumour Biol* **21**, 258–266.

[12] Miyazaki J, Hokari R, Kato S, Tsuzuki Y, Kawaguchi A, Nagao S, Itoh K, and Miura S (2002). Increased expression of galectin-3 in primary gastric cancer and the metastatic lymph nodes. *Oncol Rep* **9**, 1307–1312.

[13] Nakamura M, Inufusa H, Adachi T, Aga M, Kurimoto M, Nakatani Y, Wakano T, Nakajima A, Hida JI, Miyake M, et al. (1999). Involvement of galectin-3 expression in colorectal cancer progression and metastasis. *Int J Oncol* **15**, 143–148.

[14] Shekhar MP, Nangia-Makker P, Tait L, Miller F, and Raz A (2004). Alterations in galectin-3 expression and distribution correlate with breast cancer progression: functional analysis of galectin-3 in breast epithelial–endothelial interactions. *Am J Pathol* **165**, 1931–1941.

[15] Cindolo L, Benvenuto G, Salvatore P, Pero R, Salvatore G, Mirone V, Prezioso D, Altieri V, Bruni CB, and Chiariotti L (1999). Galectin-1 and galectin-3 expression in human bladder transitional-cell carcinomas. *Int J Cancer* **84**, 39–43.

[16] Feilchenfeldt J, Totsch M, Sheu SY, Robert J, Spiliopoulos A, Frilling A, Schmid KW, and Meier CA (2003). Expression of galectin-3 in normal and malignant thyroid tissue by quantitative PCR and immunohistochemistry. *Mod Pathol* **16**, 1117–1123.

[17] Inohara H, Akahani S, and Raz A (1998). Galectin-3 stimulates cell proliferation. *Exp Cell Res* **245**, 294–302.

[18] Yang RY and Liu FT (2003). Galectins in cell growth and apoptosis. *Cell Mol Life Sci* **60**, 267–276.

[19] Glinsky VV, Glinsky GV, Glinskii OV, Huxley VH, Turk JR, Mossine VV, Deutscher SL, Pienta KJ, and Quinn TP (2003). Intravascular metastatic cancer cell homotypic aggregation at the sites of primary attachment to the endothelium. *Cancer Res* **63**, 3805–3811.

[20] Glinsky VV, Glinsky GV, Rittenhouse-Olson K, Huflejt ME, Glinskii OV, Deutscher SL, and Quinn TP (2001). The role of Thomsen-Friedenreich antigen in adhesion of human breast and prostate cancer cells to the endothelium. *Cancer Res* **61**, 4851–4857.

[21] Khaldoyanidi SK, Glinsky VV, Sikora L, Glinskii AB, Mossine VV, Quinn TP, Glinsky GV, and Sriramarao P (2003). MDA-MB-435 human breast carcinoma cell homo- and heterotypic adhesion under flow conditions is mediated in part by Thomsen-Friedenreich antigen–galectin-3 interactions. *J Biol Chem* **278**, 4127–4134.

[22] Takenaka Y, Fukumori T, and Raz A (2004). Galectin-3 and metastasis. *Glycoconj J* **19**, 543–549.

[23] Nakahara S, Oka N, and Raz A (2005). On the role of galectin-3 in cancer apoptosis. *Apoptosis* **10**, 267–275.

[24] Fukumori T, Oka N, Takenaka Y, Nangia-Makker P, Elsamman E, Kasai T, Shono M, Kanayama HO, Ellerhorst J, Lotan R, et al. (2006). Galectin-3 regulates mitochondrial stability and antiapoptotic function in response to anticancer drug in prostate cancer. *Cancer Res* **66**, 3114–3119.

[25] Takenaka Y, Fukumori T, Yoshii T, Oka N, Inohara H, Kim HR, Bresalier RS, and Raz A (2004). Nuclear export of phosphorylated galectin-3 regulates its antiapoptotic activity in response to chemotherapeutic drugs. *Mol Cell Biol* **24**, 4395–4406.

[26] Yu F, Finley RL Jr, Raz A, and Kim HR (2002). Galectin-3 translocates to the perinuclear membranes and inhibits cytochrome *c* release from the mitochondria. A role for synexin in galectin-3 translocation. *J Biol Chem* **277**, 15819–15827.

[27] Honjo Y, Nangia-Makker P, Inohara H, and Raz A (2001). Down-regulation of galectin-3 suppresses tumorigenicity of human breast carcinoma cells. *Clin Cancer Res* **7**, 661–668.

[28] Nangia-Makker P, Sarvis R, Visscher DW, Bailey-Penrod J, Raz A, and Sarkar FH (1998). Galectin-3 and L1 retrotransposons in human breast carcinomas. *Breast Cancer Res Treat* **49**, 171–183.

[29] Nangia-Makker P, Honjo Y, Sarvis R, Akahani S, Hogan V, Pienta KJ, and Raz A (2000). Galectin-3 induces endothelial cell morphogenesis and angiogenesis. *Am J Pathol* **156**, 899–909.

[30] Pienta KJ, Naik H, Akhtar A, Yamazaki K, Replogle TS, Lehr J, Donat TL, Tait L, Hogan V, and Raz A (1995). Inhibition of spontaneous metastasis in a rat prostate cancer model by oral administration of modified citrus pectin. *J Natl Cancer Inst* **87**, 348–353.

[31] Nangia-Makker P, Hogan V, Honjo Y, Baccarini S, Tait L, Bresalier R, and Raz A (2002). Inhibition of human cancer cell growth and metastasis in nude mice by oral intake of modified citrus pectin. *J Natl Cancer Inst* **94**, 1854–1862.

[32] Glinsky GV, Mossine VV, Price JE, Bielenberg D, Glinsky VV, Ananthaswamy HN, and Feather MS (1996). Inhibition of colony formation in agarose of metastatic human breast carcinoma and melanoma cells by synthetic glycoamine analogs. *Clin Exp Metastasis* **14**, 253–267.

[33] Glinsky GV, Price JE, Glinsky VV, Mossine VV, Kiriakova G, and Metcalf JB (1996). Inhibition of human breast cancer metastasis in nude mice by synthetic glycoamines. *Cancer Res* **56**, 5319–5324.

[34] Arbiser JL, Moses MA, Fernandez CA, Ghiso N, Cao Y, Klauber N, Frank D, Brownlee M, Flynn E, Parangi S, et al. (1997). Oncogenic H-ras stimulates tumor angiogenesis by two distinct pathways. *Proc Natl Acad Sci USA* **94**, 861–866.

[35] Chauhan D, Li G, Podar K, Hideshima T, Neri P, He D, Mitsiades N, Richardson P, Chang Y, Schindler J, et al. (2005). A novel carbohydrate-based therapeutic GCS-100 overcomes bortezomib resistance and enhances dexamethasone-induced apoptosis in multiple myeloma cells. *Cancer Res* **65**, 8350–8358.

[36] Glinskii OV, Huxley VH, Glinsky GV, Pienta KJ, Raz A, and Glinsky VV (2005). Mechanical entrapment is insufficient and intercellular adhesion is essential for metastatic cell arrest in distant organs. *Neoplasia* **5**, 522–527.

[37] Cengel KA, Voong KR, Chandrasekaran S, Maggiorella L, Brunner TB, Stanbridge E, Kao GD, McKenna WG, and Bernhard EJ (2007). Oncogenic K-Ras signals through epidermal growth factor receptor and wild-type H-Ras to promote radiation survival in pancreatic and colorectal carcinoma cells. *Neoplasia* **9**, 341–348.

[38] Kock N, Kasmieh R, Weissleder R, and Shah K (2007). Tumor therapy mediated by lentiviral expression of shBcl-2 and S-TRAIL. *Neoplasia* **9**, 435–442.

[39] Trudel S, Stewart AK, Li Z, Shu Y, Liang SB, Trieu Y, Reece D, Paterson J, Wang D, and Wen XY (2007). The Bcl-2 family protein inhibitor, ABT-737, has substantial antimyeloma activity and shows synergistic effect with dexamethasone and melphalan. *Clin Cancer Res* **13**, 621–629.

[40] Heimburg J, Yan J, Morey S, Wild L, Glinskii OV, Huxley VH, Klick R, Roy R, Glinsky VV, and Rittenhouse-Olson K (2006). Inhibition of spontaneous breast cancer metastasis by anti–Thomsen-Friedenreich antigen monoclonal antibody JAA-F11. *Neoplasia* **8**, 939–948.

[41] Webster JD, Yuzbasiyan-Gurkan V, Kaneene JB, Miller R, Resau JH, and Kiupel M (2006). The role of c-KIT in tumorigenesis: evaluation in canine cutaneous mast cell tumors. *Neoplasia* **8**, 104–111.